Synthesis, Characterization, and Electrochemistry of *cis*-Oxothio- and *cis*-Bis(thio)tungsten(VI) Complexes of Hydrotris(3,5-dimethylpyrazol-1-yl)borate

Aston A. Eagle,[1a] Edward R. T. Tiekink,[1b] Graham N. George,[1c] and Charles G. Young*,[1a]

School of Chemistry, University of Melbourne, Victoria 3010, Australia, Department of Chemistry, University of Adelaide, Adelaide, South Australia 5005, Australia, and Stanford Synchrotron Radiation Laboratory, SLAC, PO Box 4349, MS 69, Stanford, California 94309

Received January 23, 2001

The complexes Tp*WO_2X react with sulfiding agents such as B_2S_3 or P_4S_{10} to give the oxothio- and bis(thio)-tungsten(VI) complexes Tp*WOSX (X = Cl^-) and Tp*WS_2X [X = Cl^-, $S_2PPh_2^-$; Tp* = hydrotris(3,5-dimethylpyrazol-1-yl)borate]. The reaction of Tp*WS_2Cl with (i) PPh_3 in pyridine and (ii) dimethyl sulfoxide affords Tp*WOSCl in good overall yield. The chloro complexes undergo metathesis with alkali metal salts to yield species of the type Tp*WOSX and Tp*WS_2X [X = OPh^-, SPh^-, $SePh^-$, (−)-mentholate]. The diamagnetic complexes exhibit NMR spectra indicative of C_1 (Tp*WOSX) or C_s (Tp*WS_2X) symmetry and IR spectra consistent with terminal oxo and thio ligation (ν(W═O), 940−925 cm^{-1}; ν(W═S) or $\nu(WS_2)$, 495−475 cm^{-1}). Crystals of (*R*,*S*)-Tp*WOS{(−)-mentholate} are monoclinic, space group $P2_1$, with a = 11.983(2) Å, b = 18.100(3) Å, c = 13.859(3) Å, β = 91.60(2) °, V = 3004.6(8) $Å^3$, and Z = 4. Crystals of Tp*$WS_2(OPh)\cdot CH_2Cl_2$ are orthorhombic, space group *Pbca*, with a = 16.961(4) Å, b = 33.098(7) Å, c = 9.555(2) Å, V = 5364(2) $Å^3$, and Z = 8. The mononuclear, distorted-octahedral tungsten centers are coordinated by a tridentate Tp* ligand, an alkoxy or aryloxy ligand, and two terminal chalcogenide ligands. The average W═O and W═S distances are 1.726(7) and 2.125(2) Å, respectively, and the O═W═S and S═W═S angles 102.9(3) and 102.9(1)°, respectively. The tungsten and sulfur X-ray absorption spectra of Tp*WOSCl and Tp*WS_2Cl are consistent with the presence of terminal π-bonded thio ligands in both complexes. The thio complexes generally undergo a reversible one-electron reduction at potentials significantly more positive than their oxo analogues. The chemical, spectroscopic, and electrochemical properties of the complexes are heavily influenced by the presence of W═S π* frontier orbitals.

Introduction

Transition metal−sulfur centers catalyze a number of very important chemical reactions in industry and biology.[2−5] In the petroleum industry, Ni- and Co-promoted Mo and W sulfides are widely employed as hydrotreating catalysts for the removal of sulfur (hydrodesulfurization), nitrogen, oxygen, and metals from refinery feedstocks.[2,4−9] Metal sulfides also find applications as isomerization, dehydration, and hydrocracking catalysts, as lubricants, and in semiconductor, photocatalytic, and electrocatalytic devices.[2,4,5] Hydrodesulfurization mechanisms frequently invoke the generation of bridging and terminal thio and hydrosulfido (protonated thio, SH^-) ligands during catalysis.[2,4−9]

In biological systems,[2−4] Mo− and W−S centers comprise the active sites of nitrogenase[10] and the many pterin-containing molybdenum[11] and tungsten[12] enzymes. Thio and hydrosulfido ligands are a feature of the Mo(VI), -(V), and -(IV) states of xanthine oxidase and aldehyde oxidase, which catalyze the activation and hydroxylation of substrate C−H bonds.[11] Very recently, a broad synthetic model for enzyme centers of this type was reported.[13] A number of tungsten enzymes, having key roles in the assimilation of carbon from CO_2, proteins, and carbohydrates by hyperthermophilic organisms, are also known.[12] The aldehyde ferredoxin oxidoreductase from *Pyrococcus furiosus* contains a mononuclear bis(molybdopterin)−W active

(1) (a) University of Melbourne. (b) University of Adelaide. Present address: Department of Chemistry, National University of Singapore, Singapore, 117543. (c) Stanford Synchrotron Radiation Laboratory.
(2) *Sulfur. Its Significance for Chemistry, for the Geo-, Bio- and Cosmosphere and Technology*; Müller, A., Krebs, B., Eds.; Elsevier: Amsterdam, 1984.
(3) *Molybdenum Enzymes, Cofactors, and Model Systems*, Stiefel, E. I., Coucouvanis, D., Newton, W. E., Eds.; ACS Symposium Series 535; American Chemical Society: Washington, DC, 1993.
(4) *Transition Metal Sulfur Chemistry; Biological and Industrial Significance*; Stiefel, E. I., Matsumoto, K., Eds.; ACS Symposium Series 653; American Chemical Society: Washington, DC, 1996.
(5) Stiefel, E. I. In *Kirk-Othmer Encyclopedia of Chemical Technology*, 4th ed.; Wiley: New York, 1995; Vol. 16, pp 940−962.
(6) Chianelli, R. R.; Daage, M.; Ledoux, M. J. *Adv. Catal.* **1994**, *40*, 177.
(7) Topsøe, H.; Clausen, B. S.; Massoth, F. E. *Hydrotreating Catalysis: Science and Technology*, Springer-Verlag: Berlin, 1996.
(8) Angelici, R. J. In *Encyclopedia of Inorganic Chemistry*; King, R. B., Ed.; Wiley: Chichester, U.K., 1994; p 1433.
(9) Curtis, M. D. In *Transition Metal Sulfur Chemistry; Biological and Industrial Significance*; Stiefel, E. I., Matsumoto, K., Eds.; ACS Symposium Series 653; American Chemical Society: Washington, DC, 1996; p 154.
(10) (a) Chan, M. K.; Kim, J.; Rees, D. C. *Science* **1993**, *260*, 792. (b) Stiefel, E. I.; George, G. N. In *Bioinorganic Chemistry*; Bertini, I.; Gray, H. B., Lippard, S. J., Valentine, J. S., Eds.; University Science Books: Mill Valley, CA, 1994; Chapter 7, p 365. (c) Howard, J. B.; Rees, D. C. *Chem. Rev.* **1996**, *96*, 2965. (d) Burgess, B. K.; Lowe, D. J. *Chem. Rev.* **1996**, *96*, 2983.
(11) (a) Pilato, R. S.; Stiefel, E. I. In *Inorganic Catalysis*; Reedijk, J., Bouwman, E. Eds.; Marcel Dekker: New York, 1999; p 81. (b) Enemark, J. H.; Young, C. G. *Adv. Inorg. Chem.* **1993**, *40*, 1. (c) Young, C. G.; Wedd, A. G. *Encyclopedia of Inorganic Chemistry*; King, R. B., Ed.; Wiley: New York, 1994; p 2330. (d) Hille, R. *Chem. Rev.* **1996**, *96*, 2757.
(12) (a) Kletzin, A.; Adams, M. W. W. *FEMS Microbiol. Rev.* **1996**, *18*, 5. (b) Johnson, M. K.; Rees, D. C.; Adams, M. W. W. *Chem. Rev.* **1996**, *96*, 2817.
(13) Smith, P. D.; Slizys, D. A.; George, G. N.; Young, C. G. *J. Am. Chem. Soc.* **2000**, *122*, 2946.

10.1021/ic010084s CCC: $20.00
Published on Web 07/27/2001

site, but the nature of the other ligands remains uncertain.[14] EXAFS and inactivation (cyanide or arsenite)−reactivation (sulfide) studies suggest that the active site of the enzyme may contain thio or hydrosulfido ligands.[15] More recent EPR and variable-temperature MCD studies support the possible existence of a thio−W(VI) center in some forms of the enzymes.[16,17] The replacement of an oxo ligand by a thio ligand increases the redox potentials of Mo(VI) complexes[18] and enzymes;[11] this implicates a redox role for thio ligation at enzyme (Mo and, by extension, W) active sites. Thus, in both industrial and biological systems there is either direct or indirect evidence for the involvement of thio− or hydrosulfido−Mo and −W centers in catalysis; a better understanding of thio−Mo and −W chemistry would underpin progress in both areas.

Oxo complexes dominate the high-valent chemistry of molybdenum[19,20] and tungsten,[20,21] but stable mononuclear thio complexes are relatively rare, being more prevalent for tungsten than for molybdenum.[22] *cis*-Oxothiotungsten species are particularly uncommon yet these may prove to be the most relevant from a biological perspective; examples include $[WO_{4-n}S_n]^{2-}$ ($n = 1-3$),[23] $WOS(ONR_2)_2$,[24] $(PPh_4)_2[WOS(NCS)_4]$,[25] Cp*WOSR (R = Me, CH_2SiMe_3,[26,27] S^tBu[28]), $(L-N_2S_2)WOS$,[29] and, more recently, $WOS(OSiPh_3)_2(Me_4phen)$.[30] Of these, only $(PPh_4)_2[WOS(NCS)_4]$[25] and $WOS(OSiPh_3)_2(Me_4phen)$[30] have been structurally characterized, although the latter is disordered. *cis*-Bis(thio)tungsten complexes are just as unusual,[28−34] and few have been structurally characterized.[28−30,33,34]

We have been exploring thiotungsten chemistry with the 2-fold aim of (i) expanding the limited chemistry of mononuclear species containing oxo−thio and bis(thio) π-base ligand combinations and (ii) providing chemical, spectroscopic, and electrochemical insights which may inform the interpretation of enzyme studies. Over recent years we have developed complementary high-valent[32−34] and low-valent[33,34] approaches for the synthesis of mononuclear oxothio- and bis(thio)tungsten(VI) complexes containing the sterically demanding hydrotris(3,5-dimethylpyrazol-1-yl)borate ligand (Tp*). This ligand has been used to maintain the mononuclearity of the metal center and restrict the potential thio-ligand chemistry to three mutually cis (fac) coordination sites. This paper reports high-valent syntheses for a wide variety of oxothio- and bis(thio)tungsten(VI) complexes of the type Tp*WOSX and Tp*WS_2X (X = Cl^-, OPh^-, SPh^-, $SePh^-$, (−)-mentholate, $S_2PPh_2^-$), spectroscopic, structural, and electrochemical studies of the compounds, and aspects of their reactivity and electronic structure.

Experimental Section

Materials and Methods. The compounds KTp*,[35] $[WOSCl_2]_n$,[36] Tp*WO_2Cl,[32,37] and Tp*$WO_2(S_2PPh_2)$[37] were prepared by literature methods. Sodium salts were prepared by reaction of the free acids with 1 equiv of NaOH in methanol (NaOPh, NaSPh) or sodium in refluxing tetrahydrofuran (sodium (−)-mentholate). Boron sulfide (Johnson-Matthey), $(Me_3Si)_2S$ (Fluka), 18-crown-6, Ph_2Se_2, and P_4S_{10} (Aldrich) were used as obtained from suppliers. Unless stated, all reactions were performed under an atmosphere of pure dinitrogen employing standard Schlenk techniques, but workups were performed in air. Solvents were carefully dried and deoxygenated before use. Unless otherwise specified, chromatography was performed on 50 cm × 2 cm diameter Merck Art. 7734 Keiselgel 60 columns using 3/2 CH_2Cl_2/hexane as eluent.

Infrared spectra were recorded on a Perkin-Elmer 1430 spectrophotometer as pressed KBr disks. Proton NMR spectra were obtained using a Varian FT Unity-300 spectrometer and were referenced to internal $CHCl_3$ (δ_H 7.23). EPR spectra were recorded on a Bruker FT ECS-106 spectrometer using 1,1-diphenyl-2-picrylhydrazyl as reference. Electronic spectra were obtained on Shimadzu UV-240 and Hitachi 150-20 UV spectrophotometers. Electrochemical experiments were performed using a Cypress Electrochemical System II with a 3 mm glassy carbon working electrode and platinum auxiliary and reference electrodes. Solutions of the complexes (1−2 mM) in 0.1 M $NBu^n_4BF_4$/acetonitrile were employed and potentials were referenced to internal ferrocene ($E_{1/2}$ = +0.390 V vs SCE). Potentials are reported relative to the saturated calomel electrode (SCE). Mass spectra were recorded on a Vacuum Generators VG ZAB 2HF mass spectrometer. Microanalyses were performed by Atlantic Microlabs, Norcross, GA. Characterization data are summarized in Table 1. A complete listing of infrared spectral bands is included in the Supporting Information.

Syntheses. Tp*WOSCl. Method 1. A suspension of Tp*WO_2Cl (2.00 g, 3.65 mmol) and B_2S_3 (0.44 g, 3.7 mmol) in benzene (50 mL) was refluxed for 4 d. Fresh B_2S_3 (0.88 g, 7.5 mmol) was then added and the mixture refluxed for a further 2 d. Following removal of the

(14) Chan, M. K.; Mukund, S.; Kletzin, A.; Adams, M. W. W.; Rees, D. C. *Science* **1995**, *267*, 1463.
(15) (a) Mukund, S.; Adams, M. W. W. *J. Biol. Chem.* **1990**, *265*, 11508. (b) Mukund, S.; Adams, M. W. W. *J. Biol. Chem.* **1991**, *266*, 14208. (c) George, G. N. Unpublished work.
(16) Koehler, B. P.; Mukund, S.; Conover, R. C.; Dhawan, I. K.; Roy, R.; Adams, M. W. W.; Johnson, M. K. *J. Am. Chem. Soc.* **1996**, *118*, 12391.
(17) Dhawan, I. K.; Roy, R.; Koehler, B. P.; Mukund, S.; Adams, M. W. W.; Johnson, M. K. *J. Biol. Inorg. Chem.* **2000**, *5*, 313.
(18) (a) Bristow, S.; Garner, C. D.; Pickett, C. J. *J. Chem. Soc., Dalton Trans.* **1984**, 1617. (b) Traill, P. R.; Bond, A. M.; Wedd, A. G. *Inorg. Chem.* **1994**, *33*, 5754.
(19) For reviews see: (a) Stiefel, E. I. *Prog. Inorg. Chem.* **1977**, *22*, 1. (b) Garner, C. D.; Charnock, J. M. In *Comprehensive Coordination Chemistry*; Wilkinson, G., Gillard, R. D., McCleverty, J. A., Eds.; Pergamon: Oxford, U.K., 1987; Chapter 36.4, p 1329. (c) Stiefel, E. I. In *Comprehensive Coordination Chemistry*; Wilkinson, G., Gillard, R. D., McCleverty, J. A., Eds.; Pergamon: Oxford, U.K., 1987; Chapter 36.5, p 1375.
(20) Parkin, G. *Prog. Inorg. Chem.* **1998**, *47*, 1.
(21) For reviews see: (a) Dori, Z. *Prog. Inorg. Chem.* **1981**, *28*, 239. (b) Dori, Z. In *Comprehensive Coordination Chemistry*; Wilkinson, G., Gillard, R. D., McCleverty, J. A., Eds.; Pergamon: Oxford, U.K., 1987; Chapter 37, p 973.
(22) Orpen, A. G.; Brammer, L.; Allen, F. H.; Kennard, O.; Watson, D. G.; Taylor, R. *J. Chem. Soc., Dalton Trans.* **1989**, S1.
(23) (a) Diemann, E.; Müller, A. *Coord. Chem. Rev.* **1973**, *10*, 79. (b) Müller, A.; Diemann, E.; Jostes, R.; Bögge, H. *Angew. Chem., Int. Ed. Engl.* **1981**, *20*, 934.
(24) McDonell, A. C.; Vasudevan, S. G.; O'Connor, M. J.; Wedd, A. G. *Aust. J. Chem.* **1985**, *38*, 1017.
(25) Potvin, C.; Manoli, J. M.; Marzak, S.; Secheresse, F. *Acta Crystallogr.* **1988**, *C44*, 369.
(26) Faller, J. W.; Ma, Y. *Organometallics* **1989**, *8*, 609.
(27) Abbreviations: Bz = benzyl; Cp = η^5-cyclopentadienyl; Cp* = η^5-pentamethylcyclopentadienyl; DMF = *N*,*N*-dimethylformamide; edt = ethane-1,2-dithiolate; Fc = ferrocene; $L-N_2S_2$ = dianion of *N*,*N*′-dimethyl-*N*,*N*′-bis(2-mercaptophenyl)-1,2-diaminoethane; Me_4phen = 3,4,7,8-tetramethyl-1,10-phenanthroline; py = pyridine; Tp* = hydrotris(3,5-dimethylpyrazol-1-yl)borate; Tp^{Pr} = hydrotris(3-isopropylpyrazol-1-yl)borate (note: in previous articles describing related chemistry we have used the abbreviations L and L^{Pr} for the aforementioned Tp*/Tp^{Pr} ligands).
(28) (a) Kawaguchi, H.; Tatsumi, K. *J. Am. Chem. Soc.* **1995**, *117*, 3885. (b) Kawaguchi, H.; Yamada, K.; Lang, J.-P.; Tatsumi, K. *J. Am. Chem. Soc.* **1997**, *119*, 10346.
(29) Barnard, K. R.; Gable, R. W.; Wedd, A. G. *J. Biol. Inorg. Chem.* **1997**, *2*, 623.
(30) Miao, M.; Willer, M. W.; Holm, R. H. *Inorg. Chem.* **2000**, *39*, 2843.
(31) Yu, S.-B.; Holm, R. H. *Inorg. Chem.* **1989**, *28*, 4385.
(32) Eagle, A. A.; Tiekink, E. R. T.; Young, C. G. *J. Chem. Soc., Chem. Commun.* **1991**, 1746.
(33) Eagle, A. A.; Harben, S. M.; Tiekink, E. R. T.; Young, C. G. *J. Am. Chem. Soc.* **1994**, *116*, 9749.
(34) Eagle, A. A.; Thomas, S.; Young, C. G. In *Transition Metal Sulfur Chemistry: Biological and Industrial Significance*; Stiefel, E. I., Matsumoto, K., Eds.; ACS Symposium Series No. 653; American Chemical Society: Washington, DC, 1996; Chapter 20, pp 324−335.
(35) Trofimenko, S. *J. Am. Chem. Soc.* **1967**, *89*, 6288.
(36) Gibson, V. C.; Kee, T. P.; Shaw, A. *Polyhedron* **1990**, *9*, 2293.
(37) Eagle, A. A.; Tiekink, E. R. T.; Young, C. G. *Inorg. Chem.* **1997**, *36*, 6315.

Table 1. Characterization Data for Tp*WOSX and Tp*WS_2X Complexes

		IR spectrum (KBr, cm^{-1})			^{1}H NMR spectrum, δ (multiplicity, no. of H) ($CDCl_3$)			elect. spectrum (CH_2Cl_2)
compd (color)	m/z $[M]^{+a}$	ν(BH)	$\nu(WE_2)^b$	X ligand	Tp*(methyl)^c	Tp*(methine)^d	X ligand	λ_{max} nm (ϵ, $M^{-1}\cdot cm^{-1}$)
Tp*WOSCl (pink)	565 (3%)	2560 m	940 s, 480 s	ν(WCl) 340 s	2.33, 2.37, 2.41	5.81, 5.95		530 (45)
					2.59, 2.68, 2.93	5.98		
Tp*WOS(OPh) (orange/red)	622 (41%)	2550 m	935 s, 480 s	1590 s, 1490 s	2.17, 2.36, 2.41	5.75, 5.95	7.02 (t, 1H), 7.26 (d, 2H)	420 sh (1420)
					2.44, 2.57, 2.91	5.99	7.36 (t, 2H), all *J* 7.6 Hz	
Tp*WOS(SPh) (red)	638 (17%)	2550 m	925 s, 480 s	1580 s, 1475 m	2.38, 2.40, 2.45	5.84, 5.97	7.10 (t, 1H), 7.34 (t, 2H)	500 (1095)
					2.62, 2.74, 3.00	6.02	7.80 (d, 2H), all *J* 7.5 Hz	
Tp*WOS(SePh) (brown)		2550 m	930 s, 480 s	1570 w, 1470 w	2.36, 2.38, 2.44	5.82, 5.95	7.09 (t, 1H), 7.26 (t, 2H)	542 (905)
					2.68, 2.69, 3.08	6.01	7.81 (d, 2H), all *J* 6.8 Hz	
(*R,S*)-Tp*WOSX^e (orange)	684 (3%)	2550 m	930 s, 480 s		2.33, 2.34 (9H), 2.41 (6H)	5.74 (2H), 5.88	0.70, 0.72, 0.76, 0.83,	500 (50)
					2.48, 2.49, 2.76, 2.85	5.89 (2H), 5.91	0.91, 1.00 (d, 6 × 3H, ^3J	
					2.92 (6H)		7 Hz), 1.0−2.6 (m, 18H),	
							4.21, 4.42 (dt, 2 × 1H, ^3J	
							7 Hz, ^4J 3 Hz)	
Tp*WS_2Cl (green)	580 (37%)	2550 m	495 m, 475 s	ν(WCl) 325 s	2.36 (6H), 2.39, 2.76	5.89 (2H), 6.02		455 (495), 585 (175)
					2.81 (6H)			
Tp*WS_2(OPh) (brown)	638 (37%)	2550 m	495 w, 475 s	1590 m, 1480 w	2.31 (6H), 2.40 (6H), 2.44	5.83 (2H), 6.07	7.07 (m, 1H)	485 (655)
					3.04		7.38 (m, 4H)	
Tp*WS_2(SPh) (red-brown)	654 (20%)	2550 w	495 m, 475 s	1570 w, 1470 w	2.41 (6H), 2.43, 2.77 (6H)	5.92 (2H), 6.05	7.13 (t, 1H), 7.40 (t, 2H)	445 (3540)
					2.86		7.88 (d, 2H), all *J* 7.5 Hz	
Tp*WS_2(SePh) (red)		2560 m	495 m, 475 s	1570 m, 1470 m	2.42 (9H), 2.81, 2.90 (6H)	5.94 (2H), 6.03	7.13 (t, 1H), 7.35 (t, 2H)	430 (2580), 505 (2770)
							7.94 (d, 2H), all *J* 7.5 Hz	
Tp*$WS_2(S_2PPh_2)$ (brown)	794 (20%)	2555 m	495 m, 475 s	1430 s, 525 s	2.37 (6H), 2.40, 2.62 (6H)	5.85 (2H), 6.01	7.42 (m, 6H)	485 sh (840), 640 sh (125)
					2.72		8.07 (m, 4H)	

^{a} Electron impact mass spectrometric data; peak intensities indicated by percentage relative to strongest peak at 100%. ^{b} E_2 = OS or S_2. ^{c} Singlet resonances integrating for three protons unless indicated. ^{d} Singlet resonances integrating for one proton unless indicated. ^{e} X = (−)-mentholate; the *R* and *S* isomers are present in equal quantities.

solvent by rotary evaporation, the residue was suspended in a small volume of dichloromethane and the mixture chromatographed. The first green band yields Tp*WS_2Cl (0.41 g, 19%); the second yellow band gives impure Tp*WOSCl (0.58 g, 28%).

Method 2. A mixture of Tp*WO_2Cl (1.00 g, 1.82 mmol) and P_4S_{10} (0.162 g, 0.364 mmol) in benzene (25 mL) was refluxed for 20 h, and then the solvent was removed by rotary evaporation. The residue was suspended in dichloromethane (ca. 10 mL) and the mixture chromatographed. The first green band yielded Tp*WS_2Cl (0.175 g, 17%) after recrystallization from CH_2Cl_2/hexane, while the second pink band yielded Tp*WOSCl (0.133 g, 13%), after recrystallization from CH_2Cl_2/MeOH.

Method 3. A mixture of Tp*WS_2Cl (0.100 g, 0.172 mmol) and PPh_3 (0.047 g, 0.181 mmol) in pyridine (6 mL) was stirred for 15 min, and then the resulting deep blue solution was evaporated to dryness and reconstituted with benzene (10 mL). The benzene solution was treated with dimethyl sulfoxide (20 μL, 0.28 mmol) and stirred overnight. The resulting red solution was reduced to dryness, the solid redissolved in CH_2Cl_2 (5 mL), and the new solution chromatographed. The first red band was collected, and the compound was recrystallized from CH_2Cl_2/hexane or CH_2Cl_2/MeOH, isolated by filtration, and vacuum-dried. Yield: 0.069 g (71%).

Method 4. Freshly sublimed $WOCl_4$ (1.00 g, 2.93 mmol) was converted to $[WOSCl_2]_n$ using $(Me_3Si)_2S$ (0.61 mL, 2.9 mmol).[36] The solvent was removed under vacuum, and then KTp* (0.980 g, 2.91 mmol) and CH_2Cl_2 (20 mL) were added. The mixture was stirred for 3 d, reduced in volume to 12 mL, and then chromatographed. The first red band was collected, and the product was recrystallized from CH_2Cl_2/MeOH. Yield: 0.290 g (18%).

Anal. Calcd for dichloromethane hemisolvate (confirmed by NMR), $C_{15.25}H_{22.5}BCl_{1.5}N_6OSW$: C, 31.27; H, 3.87; N, 14.35; S, 5.47; Cl, 9.08. Found: C, 31.30; H, 3.78; N, 14.46; S, 5.38; Cl, 8.94.

Tp*WOS(OPh). A mixture of Tp*WOSCl (0.100 g, 0.177 mmol), NaOPh (0.05 g, 0.43 mmol), and 18-crown-6 (5 mg) in toluene (10 mL) was refluxed for 20 h and then reduced to dryness at 70 °C. The residue was dissolved in 3/2 CH_2Cl_2/hexanes and chromatographed. The first orange band was identified by ^{1}H NMR as Tp*WS_2(OPh) (0.012 g, 21% by S). The second orange band was collected and evaporated to yield crude product. Orange-red crystals were obtained by slow diffusion of MeOH into a CH_2Cl_2 solution. Yield: 0.070 g (64%).

Anal. Calcd for $C_{21}H_{27}BN_6O_2SW$: C, 40.53; H, 4.37; N, 13.51; S, 5.15. Found: C, 40.37; H, 4.35; N, 13.43; S, 5.22.

Tp*WOS(SPh). A mixture of Tp*WOSCl (0.138 g, 0.244 mmol), NaSPh (0.10 g, 0.76 mmol), and 18-crown-6 (5 mg) in toluene (15 mL) was refluxed for 1 h and then reduced to 2 mL by rotary evaporation at 70 °C. The mixture was then eluted on a silica gel column using toluene as eluent. The first red band was collected and reduced to dryness and then redissolved in hexane and allowed to slowly evaporate to a final volume of 1 mL. The supernatant was decanted, and the resulting dark red crystalline blocks were washed with hexane (1 mL). Yield: 0.067 g (43%).

Anal. Calcd for $C_{21}H_{27}BN_6OS_2W$: C, 39.51; H, 4.26; N, 13.17; S, 10.05. Found: C, 39.61; H, 4.23; N, 13.13; S, 10.12.

Tp*WOS(SePh). A solution of Ph_2Se_2 (0.029 g, 0.093 mmol) in tetrahydrofuran (10 mL) was titrated with $LiEt_3BH$ (1.0 equiv of a 1.0 M solution in tetrahydrofuran) until the yellow color was discharged. The solvent and volatile BEt_3 were then removed by heating to 50 °C under vacuum for 20 min. The resulting residue of LiSePh was redissolved in tetrahydrofuran (10 mL) and then injected into a flask containing solid Tp*WOSCl (0.100 g, 0.177 mmol). After being stirred for 30 min, the resulting purple mixture was evaporated to dryness. The residue was dissolved in 3/2 CH_2Cl_2/hexanes and chromatographed. The product, collected as the first dark red band, was recrystallized by addition of water to a filtered acetonitrile solution. The clay-brown microcrystals were then dried under vacuum. Yield: 0.056 g (46%).

Anal. Calcd for $C_{21}H_{27}BN_6OSSeW$: C, 36.81; H, 3.97; N, 12.27; S, 4.68. Found: C, 36.60; H, 3.87; N, 12.15; S, 4.60.

(R,S)-Tp*WOS{(−)-mentholate}. A suspension of Tp*WOSCl (0.150 g, 0.266 mmol) in toluene (10 mL) was treated with a tetrahydrofuran solution of sodium (−)-mentholate (0.3 mmol in 1.0

mL), and then the mixture was stirred for 24 h. The mixture was reduced to 2 mL and eluted on a silica gel column using toluene as eluent. The product was collected as the first orange band and recrystallized from CH_2Cl_2/MeOH to give orange crystals with a 1:1 diastereomer ratio. Yield: 0.112 g (62%).

Anal. Calcd for $C_{25}H_{41}BN_6O_2SW$: C, 43.87; H, 6.04; N, 12.28; S, 4.68. Found: C, 43.63; H, 6.13; N, 12.17; S, 4.75.

Tp*WS$_2$Cl. Method 1. A mixture of Tp*WO_2Cl (1.00 g, 1.82 mmol) and B_2S_3 (1.00 g, 8.49 mmol) was refluxed in 1,2-dichloroethane (50 mL) for 5 d. The solvent was removed in vacuo, and then the solid was extracted using a minimum volume of dichloromethane. The solution was chromatographed on two equally loaded columns. Several columns were required to separate green Tp*WS_2Cl (0.074 g, 7%) from a small amount of orange crystalline Tp*$WSCl_2$ (first bands from column). A second green band from initial columns produced blue Tp*$WOCl_2$ (0.320 g, 31%), more Tp*$WSCl_2$, and Tp*WCl_3 (ca. 10−40 mg, 2−7%) upon further purification. The combined yield of Tp*$WSCl_2$ was 0.240 g (23%). Workup of the above reaction (except using 38 mL of 1,2-dichloroethane) after 20 h gave Tp*WS_2Cl (0.035 g, 3%), Tp*$WOCl_2$ (0.164 g, 16%), and Tp*$WSCl_2$ (0.143 g, 13%).

Method 2. A mixture of Tp*WO_2Cl (0.800 g, 1.46 mmol) and B_2S_3 (0.800 g, 6.79 mmol) was refluxed in benzene (30 mL) for 3 d and then filtered and reduced to dryness. The residue was extracted with a minimum volume of dichloromethane and chromatographed twice. The first green band was enriched in hexanes to give dark green crystals, yield 0.422 g (50%). The following red band produced impure Tp*WOSCl (0.165 g, 20%).

Method 3. A mixture of Tp*WO_2Cl (0.800 g, 1.46 mmol) and P_4S_{10} (0.800 g, 1.80 mmol) was refluxed in benzene for 16 h, and then the resulting green mixture was reduced to dryness. The residue was shaken with dichloromethane (3 × 20 mL) and filtered through a 1.5 cm plug of silica to remove a yellow impurity. The green filtrate was reduced until saturated and chromatograhed. The first green band was recrystallized from CH_2Cl_2/hexane and then CH_2Cl_2/EtOH. Yield: 0.330 g (39%).

Anal. Calcd for Tp*$WS_2Cl\cdot 0.25CH_2Cl_2$ (confirmed by NMR), $C_{15.25}H_{22.5}BCl_{1.5}N_6S_2W$: C, 30.43; H, 3.77; N, 13.97; S, 10.65; Cl, 8.84. Found: C, 30.31; H, 3.72; N, 13.94; S, 10.54; Cl, 9.04.

Tp*WS$_2$(OPh). A mixture of Tp*WS_2Cl (0.120 g, 0.207 mmol), NaOPh (0.100 g, 0.861 mmol), and 18-crown-6 (5 mg) was refluxed in toluene (10 mL) for 2.5 h and then reduced to dryness at 70 °C. [Overall yields were very sensitive to reaction times—typically, the reaction was constantly monitored by thin-layer chromatography (silica, 3/2 CH_2Cl_2/hexanes) and the reaction was stopped as soon as all Tp*WS_2Cl was consumed.] The brown residue was dissolved in dichloromethane (5 mL) and eluted on a silica gel column with 1/1 tetrahydrofuran/hexanes. The first, major orange band was evaporated, and the residue was dissolved in a minimum of acetonitrile and filtered through a silica gel microcolumn which was washed with acetonitrile. The volume of the solvent was reduced, and the brown product was precipitated by addition of distilled water, filtered out, and vacuum-dried. Yield: 0.077 g (58%).

Anal. Calcd for $C_{21}H_{27}BN_6OS_2W$: C, 39.51; H, 4.26; N, 13.17; S, 10.05. Found: C, 39.65; H, 4.25; N, 13.19; S, 9.97.

Tp*WS$_2$(SPh). Finely ground Tp*WS_2Cl (0.100 g, 0.172 mmol), NaSPh (0.070 g, 0.529 mmol), and 18-crown-6 (5 mg) were stirred in toluene (10 mL) for 1 h and then filtered through a short bed of silica gel and washed with toluene (4 × 5 mL). The orange filtrate was evaporated at 70 °C, and the residue was dissolved in acetonitrile and filtered through a silica gel microcolumn. The product was precipitated as red-brown needles by dropwise addition of water to this solution. The crystals were filtered out and then vacuum-dried. Yield: 0.093 g (83%).

Anal. Calcd for $C_{21}H_{27}BN_6S_3W$: C, 38.55; H, 4.16; N, 12.85; S, 14.70. Found: C, 38.61; H, 4.18; N, 12.89; S, 14.70.

Tp*WS$_2$(SePh). A stirred tetrahydrofuran solution (5 mL) of Ph_2Se_2 (0.066 g, 0.211 mmol) was treated with a tetrahydrofuran solution of $LiEt_3BH$ (1 equiv) until the yellow color was discharged. The solvent was evaporated and the residue heated under vacuum at 50 °C for 20 min. The resulting LiSePh was redissolved in tetrahydrofuran (10 mL) and injected into a flask containing Tp*WS_2Cl (0.235 g, 0.405 mmol). A deep burgundy color rapidly developed. After the solution was stirred for 1 h, the solvent was removed under vacuum and the residue dissolved in 3/2 CH_2Cl_2/hexanes. The solution was chromatographed on silica gel using the same solvent was eluent. Evaporation of the first red band, followed by two sucessive trituration/evaporation steps with hexane, afforded burgundy red microcrystals of product. Yield: 0.236 g (83%).

Anal. Calcd for $C_{21}H_{27}BN_6S_2SeW$: C, 35.97; H, 3.88; N, 11.99; S, 9.14. Found: C, 36.25; H, 3.87; N, 11.80; S, 9.31.

Tp*WS$_2$(S$_2$PPh$_2$). A mixture of Tp*$WO_2(S_2PPh_2)$ (0.725 g, 0.951 mmol) and B_2S_3 (0.50 g, 4.2 mmol) was refluxed in benzene (15 mL) for 19 h, and then the solvent was removed by rotary evaporation. The residue was extracted into dichloromethane (10 mL) and chromatographed. The first dark yellow band was collected and recrystallized from CH_2Cl_2/MeOH to give brown crystals. Yield: 0.31 g (41%).

Anal. Calcd for $C_{27}H_{32}BN_6PS_4W$: C, 40.82; H, 4.06; N, 10.58; S, 16.14. Found: C, 40.75; H, 4.04; N, 10.51; S, 16.14.

Table 2. Crystallographic Data

param	(*R*,*S*)-Tp*WOS{(−)-mentholate}	Tp*$WS_2(OPh)\cdot CH_2Cl_2$
formula	$C_{25}H_{41}BN_6O_2SW$	$C_{22}H_{29}BCl_2N_6OS_2W$
fw	684.4	723.2
cryst system	monoclinic	orthorhombic
space group	$P2_1$	Pbca
a, Å	11.983(2)	16.961(4)
b, Å	18.100(3)	33.098(7)
c, Å	13.859(3)	9.555(2)
β, deg	91.60(2)	90
V, Å^3	3004.6(8)	5364(2)
Z	4	8
ρ_{calcd}, g·cm^{-3}	1.513	1.791
R	0.037	0.049
R_w	0.046	0.048

[a] $R = \sum||F_o| - |F_c||/\sum|F_o|$; $R_w = [\sum w(|F_o| - |F_c|)^2/\sum(w|F_o|^2)]^{1/2}$.

Crystal Structures. Orange-red crystals of (*R*,*S*)-Tp*WOS{(−)-mentholate} and brown crystals of Tp*$WS_2(OPh)\cdot CH_2Cl_2$ were grown by diffusion of methanol into dichloromethane solutions of the complexes. Intensity data were collected at room temperature on a Rigaku AFC6R diffractometer fitted with Mo Kα radiation. Using the ω:2θ scan technique, 5959 data with θ_{max} 25.3 ° were collected for (*R*,*S*)-Tp*WOS{(−)-mentholate} and 7134 data with θ_{max} 27.9 ° were collected for Tp*$WS_2(OPh)\cdot CH_2Cl_2$. Corrections were applied for Lorentz and polarization effects,[38] and an empirical absorption correction was applied.[39] The structures were solved by direct methods[40] and refined by a full-matrix least-squares procedure based on F [38] for 4601 and 2922 data with $I = 3.0\sigma(I)$ for (*R*,*S*)-Tp*WOS{(−)-mentholate} and Tp*$WS_2(OPh)\cdot CH_2Cl_2$, respectively. Generally, non-H atoms were refined anisotropically and H atoms included in their calculated positions. The C(10) atom in (*S*)-Tp*WOS{(−)-mentholate} had high thermal motion, but multiple positions could not be resolved; this atom was refined isotropically. The B atom in Tp*WS_2(OPh) was found to be disordered over two positions of equal weight. The absolute structure of (*R*,*S*)-Tp*WOS{(−)-mentholate} was determined on the basis of the configuration of (−)-mentholate. Crystallographic data are summarized in Table 2, selected bond distances and angles are presented in Tables 3 and 4, and ORTEP[41] diagrams for the two structures are given in Figures 1 and 2.

X-ray Absorption Spectroscopy. Data Collection. X-ray absorption spectroscopy was carried out at the Stanford Synchrotron Radiation Laboratory with the SPEAR storage ring containing 60−100 mA at 3.0 GeV. Tungsten L_{III} edge spectra were collected on beamline 7-3 using an Si(220) double-crystal monochromator with an upstream vertical aperture of 1 mm and a wiggler field of 1.8 T. Harmonic

(38) *teXsan: Structure Analysis Software*; Molecular Structure Corp.: The Woodlands, TX.
(39) Walker, N.; Stuart, D. *Acta Crystallogr., Sect. A* **1983**, *39*, 158.
(40) Sheldrick, G. M. SHELX86, *Program for the Automatic Solution of Crystal Structure*; University of Göttingen: Göttingen, Germany, **1986**.
(41) Johnson, C. K. *ORTEP*; Report ORNL-5138; Oak Ridge National Laboratory: Oak Ridge, TN, 1976.

Table 3. Selected Bond Distances (Å) and Angles (deg) for (*R,S*)-Tp*WOS{(−)-mentholate}[a]

dist/angle	*S*-isomer	*R*-isomer	dist/angle	*S*-isomer	*R*-isomer
W−S(1)	2.102(5)	2.132(5)	W−O(1)	1.74(1)	1.714(9)
W−O(2)	1.835(8)	1.858(7)	W−N(11)	2.22(1)	2.26(1)
W−N(21)	2.341(9)	2.31(1)	W−N(31)	2.21(1)	2.184(9)
O(2)−C(1)	1.35(2)	1.39(2)			
S(1)−W−O(1)	103.8(4)	102.0(4)	S(1)−W−O(2)	98.9(5)	103.9(4)
S(1)−W−N(11)	164.3(3)	165.1(3)	S(1)−W−N(21)	87.9(3)	89.2(4)
S(1)−W−N(31)	94.0(3)	92.0(4)	O(1)−W−O(2)	101.1(4)	100.5(4)
O(1)−W−N(11)	88.8(5)	88.8(4)	O(1)−W−N(21)	164.0(4)	164.7(4)
O(1)−W−N(31)	88.9(4)	87.9(4)	O(2)−W−N(11)	87.6(5)	83.8(4)
O(2)−W−N(21)	87.6(3)	86.7(4)	O(2)−W−N(31)	161.3(4)	159.9(4)
N(11)−W−N(21)	78.1(4)	78.5(4)	N(11)−W−N(31)	76.7(4)	78.1(4)
N(21)−W−N(31)	79.3(3)	81.3(4)	W−O(2)−C(1)	159(1)	134.8(8)

[a] a and b designators omitted from nonmetal atom labels of *S*- and *R*-isomers, respectively; W = W(1) and W(2) for *S*- and *R*-isomers, respectively.

Table 4. Selected Bond Distances and Angles for $Tp*WS_2(OPh)$

Bond Distances (Å)					
W−S(1)	2.131(4)	W−S(2)	2.129(4)	W−O(1)	1.889(8)
W−N(11)	2.268(8)	W−N(21)	2.272(9)	W−N(31)	2.161(9)
O(1)−C(41)	1.36(1)				

Angles (deg)			
S(1)−W−S(2)	102.9(1)	S(1)−W−O(1)	100.6(2)
S(1)−W−N(11)	166.4(3)	S(1)−W−N(21)	89.6(2)
S(1)−W−N(31)	92.4(3)	S(2)−W−O(1)	99.5(3)
S(2)−W−N(11)	89.9(3)	S(2)−W−N(21)	166.7(2)
S(2)−W−N(31)	93.5(3)	O(1)−W−N(11)	81.5(3)
O(1)−W−N(21)	82.6(3)	O(1)−W−N(31)	159.0(3)
N(11)−W−N(21)	77.3(3)	N(11)−W−N(31)	82.2(3)
N(21)−W−N(31)	81.0(3)	W−O(1)−C(41)	137.3(9)

rejection was accomplished by detuning one monochromator crystal to approximately 60% off-peak, and no specular optics were present in the beamline. X-ray absorption was measured in transmittance by using nitrogen-filled ion chambers. The spectrum of a standard tungsten foil was collected simultaneously and the energy calibrated with reference to the lowest energy L_{III} edge inflection point of the standard which was assumed to be 10 207.0 eV. Samples were diluted by grinding with boron nitride so that the maximum absorbance was approximately 2.0.

Sulfur K edge experiments were performed on beamline 6-2 using an Si(111) double-crystal monochromator and wiggler field of 1.0 T. Harmonic rejection was accomplished by using a flat nickel-coated mirror downstream of the monochromator adjusted so as to have a cutoff energy of about 4500 eV. Incident intensity was monitored using an ion chamber contained in a (flowing) helium-filled flight path. Energy resolution was optimized by decreasing the vertical aperture upstream of the monochromator and quantitatively determined to be 0.51 eV by measuring the width of the 2471.4 eV 1s → $\pi^*(3b_1)$ transition of gaseous SO_2, which corresponds to a transition to a single orbital, rather than to a band of orbitals which can be the case with solid standards.[42] X-ray absorption was monitored by recording total electron yield and the energy scale was calibrated with reference to the lowest energy peak of the sodium thiosulfate standard ($Na_2S_2O_3 \cdot 5H_2O$) which was assumed to be 2469.2 eV.[43]

Data Analysis. Data were analyzed using the EXAFSPAK suite of computer programs (http://ssrl.slac.stanford.edu/EXAFSPAK.html), and no smoothing or related operations were performed upon the data. The extended X-ray absorption fine structure (EXAFS) oscillations $\chi(k)$ were quantitatively analyzed by curve-fitting using ab initio theoretical phase and amplitude functions calculated using the program FEFF (v. 8.2) of Rehr and co-workers.[44,45] Peak positions in near-edge spectra were estimated by curve-fitting to a sum of pseudo-Voigt peaks using the program EDG_FIT (pseudo-Voigt deconvolution).[46]

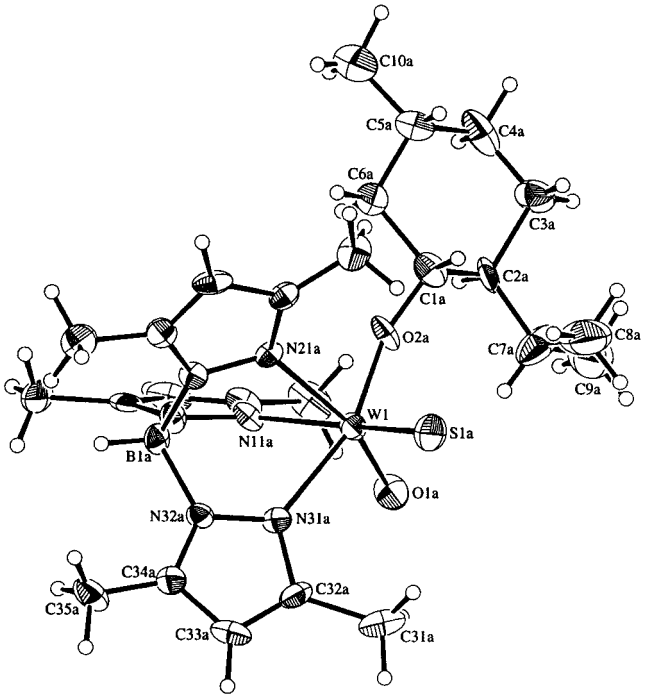

Figure 1. Molecular structure of (*S*)-Tp*WOS{(−)-mentholate}. The numbering schemes for the pyrazole rings containing N(11a) and N(21a) parallel that shown for the ring containing N(31a). Representations of the *R*-isomer have been presented elsewhere.[33,34]

Results and Discussion

Syntheses. The reaction of $Tp*WO_2Cl$ with B_2S_3 in refluxing 1,2-dichloroethane for 5−7 days produced pink Tp*WOSCl (5−10%) and green $Tp*WS_2Cl$ (7−18%).[32] The low yields are a consequence of side reactions leading to blue $Tp*WOCl_2$ (EPR: $g = 1.805$, CH_2Cl_2),[47] orange $Tp*WSCl_2$ ($g = 1.731$, CH_2Cl_2),[47] and green $Tp*WCl_3$[48] (only after 4 days) in yields of 31%, 23%, and 2−7%, respectively, after 5−7 days reflux. The byproducts are believed to form via reduction (by B_2S_3), oxo transfer (to B_2S_3), and atom transfer reactions involving the tungsten complexes and possibly solvent. Oxygen and chlorine atom transfer reactions are also a feature of the chemistry of $MCl_2(PR_3)_4$, $MOCl_3(PR_3)_2$, and $MCl_3(PR_3)_3$ (M

(42) Song, I.; Rickett, B.; Janavicius, P.; Payer, J. H.; Antonio, M. R. *Nucl. Instrum. Methods* **1995**, *A360*, 634.
(43) Sekiyama, H.; Kosugi, N.; Kuroda, H.; Ohta T. *Bull. Chem. Soc. Jpn.* **1986**, *59*, 575.
(44) Rehr, J. J.; Mustre de Leon, J.; Zabinsky, S. I.; Albers, R. C. *J. Am. Chem. Soc.* **1991**, *113*, 5135.
(45) Mustre de Leon, J.; Rehr, J. J.; Zabinsky, S. I.; Albers, R. C. *Phys. Rev.* **1991**, *B44*, 4146.
(46) Pickering, I.; George, G. N. *Inorg. Chem.* **1995**, *34*, 3142.
(47) Eagle, A. A. Ph.D. Dissertation, University of Melbourne, 1996.
(48) Millar, M.; Lincoln, S.; Koch, S. A. *J. Am. Chem. Soc.* **1982**, *104*, 288.

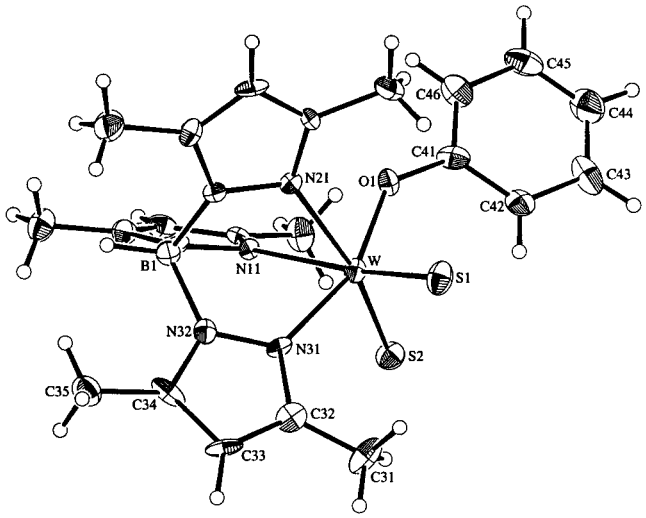

Figure 2. Molecular structure of $Tp^*WS_2(OPh)$. The numbering schemes for the pyrazole rings containing N(11) and N(21) parallel that shown for the ring containing N(31).

= Re, Mo, W; R_3 = $MePh_2$, Me_3) complexes.[49−51] The molybdenum analogue, Tp^*MoO_2Cl, reacts with sulfiding agents in refluxing 1,2-dichloroethane to form $Tp^*MoCl(S_4)$ without the detectable formation of $Tp^*MoOSCl$ or Tp^*MoS_2Cl.[52]

Improved yields of Tp^*WS_2Cl (50%) were achieved when Tp^*WO_2Cl was reacted with B_2S_3 in refluxing benzene. Blue Tp^*WOCl_2 was detected (by EPR) at early stages of the reaction but Tp^*WSCl_2 (21% based on Cl), formed by the reaction of Tp^*WOCl_2 and B_2S_3, was the only byproduct isolated after 3 days. Superior yields of Tp^*WS_2Cl were not achieved using other sulfiding agents, solvents, or reaction conditions.

Phosphorus sulfide (P_4S_{10}) was identified as an ideal substitute for B_2S_3 in the synthesis of Tp^*WOSCl and Tp^*WS_2Cl. This reagent is commonly used to prepare thioketones,[53] but it has also found some utility in the synthesis of thio complexes, e.g., in the synthesis of $[ReS(edt)_2]^-$ from $[ReO(edt)_2]^-$.[27,54] The reaction of Tp^*WO_2Cl with P_4S_{10} in refluxing benzene produces Tp^*WS_2Cl in good yield (40%) after only ca. 16 h. Phosphorus sulfide is cheaper, more readily available and effective, and induces fewer side reactions than B_2S_3. These advantages offset the marginally lower yields of Tp^*WS_2Cl from reactions involving P_4S_{10}. With both B_2S_3 and P_4S_{10}, the formation of Tp^*WS_2Cl at the expense of Tp^*WOSCl was enhanced by the use of excess sulfiding agent and prolonged reaction times. Unrecrystallized samples of Tp^*WS_2Cl prepared using P_4S_{10} occasionally contained traces of an unidentified green impurity but this did not affect subsequent reactions.

The synthesis of Tp^*WOSCl by direct sulfidation of Tp^*WO_2Cl was complicated by the simultaneous formation of Tp^*WS_2Cl, even when substoichiometric amounts of sulfiding agent were employed. This is a problem commonly encountered in the synthesis of $[MOS]^{2+}$ (M = Mo, W) complexes by sulfidation reactions.[23,24,31,55−57] The yield of Tp^*WOSCl was 5−10% from B_2S_3 in 1,2-dichloroethane,[32] 15% from P_4S_{10} in benzene, and 28% from B_2S_3 in benzene. The normal pink color of Tp^*WOSCl is masked by the presence of Tp^*WSCl_2 and an unidentified yellow byproduct in samples isolated from the benzene reaction.[58] The reaction of $[WOSCl_2]_n$ with KTp^* in dichloromethane produced pure Tp^*WOSCl, but the yield of 18% did not justify the time and cost involved in the preparation of $[WOSCl_2]_n$. The optimal synthesis of Tp^*WOSCl involved the atom transfer reactions shown in eqs 1 and 2. Thus, reaction of Tp^*WS_2Cl with PPh_3 in neat pyridine (py) produced a blue complex, presumed to be $Tp^*WSCl(py)$, which in turn reacted with dimethyl sulfoxide to afford Tp^*WOSCl in 71% yield (overall yield of 35%, based on Tp^*WO_2Cl).[32]

$$Tp^*WS_2Cl + PPh_3 + py \rightarrow Tp^*WSCl(py) + SPPh_3 \quad (1)$$

$$Tp^*WSCl(py) + Me_2SO \rightarrow Tp^*WOSCl + Me_2S + py \quad (2)$$

The complexes Tp^*WOSCl and Tp^*WS_2Cl react with MX = NaOPh, NaSPh, LiSePh, and Na{(−)-mentholate} in tetrahydrofuran (X = $SePh^-$, (−)-mentholate) or refluxing toluene/18-crown-6 (X = others) to produce Tp^*WOSX and Tp^*WS_2X, respectively. The formation of the thiotungsten(VI) derivatives was almost invariably faster than formation of analogous Tp^*WO_2X complexes,[37] and gentler conditions were usually required. While the complexes Tp^*WO_2X were generally formed more quickly with hard incoming ligands, the thiotungsten(VI) derivatives were formed more rapidly with soft incoming ligands. We were unable to prepare $Tp^*WOS(NCS)$ or $Tp^*WS_2(NCS)$ by metathesis despite prolonged reflux in toluene with 18-crown-6 and excess KNCS.

The reaction of $Tp^*WO_2(S_2PPh_2)$ with B_2S_3 in refluxing benzene for 19 h produced $Tp^*WS_2(S_2PPh_2)$ in 41% yield. This reaction mirrored the preparation of Tp^*WS_2Cl from Tp^*WO_2Cl but was only successful when B_2S_3 was used. The complex $Tp^*WOS(S_2PPh_2)$ can be synthesized from $Tp^*W^{II}(S_2PPh_2)(MeCN)(CO)$ in two sequential atom transfer reactions via $Tp^*W^{IV}E(CO)(S_2PPh_2)$ (E = O or S).[34,59]

Physical and Spectroscopic Properties. The Tp^*WOSX and Tp^*WS_2X complexes are crystalline air-stable solids, with the exception of $Tp^*WOS(SePh)$, $Tp^*WS_2(SPh)$, and $Tp^*WS_2(SePh)$, which decompose over a period of days. Solutions of the compounds are stable in air for several hours but eventually decompose; e.g., in the presence of air and methanol, $Tp^*WS_2(OPh)$ is cleanly converted to $Tp^*WO_2(OPh)$ over 1 month. The complexes Tp^*WOSX [X = Cl^-, $S_2PPh_2^-$, and (−)-mentholate] and Tp^*WS_2X (X = Cl^- and $S_2PPh_2^-$) are soluble in tetrahydrofuran and chlorinated and aromatic solvents but insoluble in diethyl ether, alcohols, alkanes, and water. The remaining complexes are very soluble in chlorinated and aromatic solvents, appreciably soluble in diethyl ether, alcohols, and alkanes, but insoluble in water. There is no evidence that these W(VI) complexes participate in internal redox reactions leading to

(49) Over, D. E.; Critchlow, S. C.; Mayer, J. M. *Inorg. Chem.* **1992**, *31*, 4643.
(50) Hall, K. A.; Mayer, J. M. *J. Am. Chem. Soc.* **1992**, *114*, 10402.
(51) Hall, K. A.; Mayer, J. M. *Inorg. Chem.* **1994**, *33*, 3289.
(52) Young, C. G.; McInerney, I. P.; Bruck, M. A.; Enemark, J. H. *Inorg. Chem.* **1990**, *29*, 412.
(53) McGregor, W. M.; Sherrington, D. C. *Chem. Soc. Rev.* **1993**, 199.
(54) Blower, P. J.; Dilworth, J. R.; Hutchinson, J. P.; Zubieta, J. A. *Inorg. Chim. Acta* **1982**, *65*, L225.
(55) (a) Hofer, E.; Holzbach, W.; Wieghardt, K. *Angew. Chem., Int. Ed. Engl.* **1981**, *20*, 282. (b) Wieghardt, K.; Hahn, M.; Weiss, J.; Swiridoff, W. *Z. Anorg. Allg. Chem.* **1982**, *492*, 164. (c) Bristow, S.; Collison, D.; Garner, C. D.; Clegg, W. *J. Chem. Soc., Dalton Trans.* **1983**, 2495.
(56) Faller, J. W.; Kucharczyk, R. R.; Ma, Y. *Inorg. Chem.* **1990**, *29*, 1662.
(57) An apparent exception is the generation of Cp^*WOSR (R = Me, Me_3SiCH_2) from the reaction of Cp^*WO_2R and H_2S.[26]
(58) The unidentified yellow product, Tp^*WOSCl, and Tp^*WSCl_2 coelute on chromatography columns. The pink/yellow color variaton in the "Tp^*WOSCl" samples is reminiscent of the behavior of "distortional isomers", which are also variable ternary mixtures: (a) Yoon, K.; Parkin, G.; Rheingold, A. L. *J. Am. Chem. Soc.* **1991**, *113*, 1437. (b) Desrochers, P. J.; Nebesny, K. W.; LaBarre, M. J.; Bruck, M. A.; Neilson, G. F.; Sperline, R. P.; Enemark, J. H.; Backes, G.; Wieghardt, K. *Inorg. Chem.* **1994**, *33*, 15.
(59) Thomas, S. Ph.D. Dissertation, University of Melbourne, 1997.

(μ-disulfido)tungsten(V) complexes, as occurs with the only known Mo analogue, $Tp^{Pr}MoOS(OPh)$.[13,27]

Microanalytical data were consistent with the formulations proposed. Mass spectra (Table 1) generally exhibited a peak cluster assignable to an $[M]^+$ ion, but only an $[M - SePh]^+$ ion was observed for selenophenolate derivatives; expected isotope patterns were observed for all peak clusters. The IR spectra of the oxo−thio complexes exhibit strong ν(W═O) (940−925 cm^{-1}) and ν(W═S) (480 cm^{-1}) bands; related complexes exhibit similar bands.[60] The IR spectra of the Tp^*WS_2X complexes exhibit $\nu_s(WS_2)$ and $\nu_{as}(WS_2)$ bands at 495 and 475 cm^{-1}, respectively.[61] The Tp* and X ligands also give rise to characteristic infrared bands (Table 1).

The point groups of the molecules, C_1 for Tp*WOSX and C_s for Tp^*WS_2X, were reflected in ^1H NMR spectra (Table 1). The Tp*WOSX complexes exhibit nine singlet resonances due to the inequivalent protonic groups of the Tp* ligand, while the Tp^*WS_2X complexes exhibit six-line spectra with 2:1 and 3:3:6:6 proton ratios for the ring methine and methyl resonances, respectively, of Tp*. As observed for complexes of the general type Tp^*ME_2X (M = Mo, W; E = O, S),[37,62] the unique methine proton resonance is deshielded relative to the other. The spectrum of (*R,S*)-Tp*WOS{(−)-mentholate} was consistent with a 1:1 ratio of the two diastereomers.

The electronic spectra of the complexes are summarized in Table 1. In general, the spectra of the orange-red oxo−thio complexes exhibited tailing (to ca. 500 nm) of intense ultraviolet bands into the visible region. The complex Tp*WOSCl exhibited a weak band at 530 nm (ϵ 45 $M^{-1}\cdot cm^{-1}$), while Tp*WOS(SPh) absorbed strongly at 500 nm (ϵ 1095 $M^{-1}\cdot cm^{-1}$). The bis(thio) complexes were generally more intensely colored than their Tp^*WO_2X and Tp*WOSX analogues. The spectra of both $Tp^*WS_2(S_2PPh_2)$ and $Tp^*WS_2(OPh)$ feature shoulders at 485 nm, while the remaining complexes exhibit discrete maxima at ca. 430−455 nm which vary in intensity from X = Cl^- (ϵ 495 $M^{-1}\cdot cm^{-1}$) to X = SPh^- (ϵ 3540 $M^{-1}\cdot cm^{-1}$). A second maximum is observed for Tp^*WS_2Cl (585 nm, ϵ 175 $M^{-1}\cdot cm^{-1}$) and $Tp^*WS_2(SePh)$ (505 nm, ϵ 2770 $M^{-1}\cdot cm^{-1}$). The intense colors of many of these formally d^0 tungsten(VI) complexes are attributed to ligand-to-metal charge-transfer transitions.

Structure of (*R,S*)-Tp*WOS{(−)-mentholate}. The two diastereomers of Tp*WOS{(−)-mentholate} could not be separated and their cocrystallization permitted the structures of both to be determined. The diastereomers are chiral at tungsten and are assigned *R*- and *S*-configurations by taking the W···B vector as the imaginary, single binding point of Tp*, which is assigned lowest priority. The remaining ligands are prioritized according to the Cahn−Ingold−Prelog rules, viz., thio > oxo > mentholate.[63] The structure of the *S*-isomer is shown in Figure 1.

The W(1)−O(1a) (1.74(1) Å), W(2)−O(1b) (1.714(9) Å), W(1)−S(1a) (2.102(5) Å), and W(2)−S(1b) (2.132(5) Å) distances are typical of W═O (average 1.692 Å) and W═S (average 2.115 Å) bonds in other compounds.[20−22,25,30] The O═W═S bond angles are only slightly different at 103.8(4) and 102.0(4)° for the *S*- and *R*- diastereomers, respectively, and are typical of angles pertaining to other *cis*-$[ME_2]^{n+}$ (E = O, S, NR, CR_2) complexes.[64] These parameters are similar to those reported for $(PPh_4)_2[WOS(NCS)_4]$ (W═O 1.715(6) Å; W═S 2.108(2) Å; O═W═S 103.3(2)°).[25] The W(1) atom of the *S*-isomer lies 0.2357(5) Å out of the plane defined by S(1a), O(2a), N(11a), and N(31a) toward the O(1a) atom (0.2084(5) Å for the *R*-isomer). The W−N bonds are lengthened in a predictable manner by the trans influence of the coligands, the W−N distances with respect to trans ligand being W═O > W═S > W−OR.

In the *R*-isomer, the mentholate isopropyl group projects away from the *cis*-$[WOS]^{2+}$ center, while these two functionalities are aligned in the *S*-isomer. Geometrically, these differences are manifested in the W/O(2)/C(1)/C(2) torsion angles of 92(3) and −178(1)°, respectively, and in the W−O−C angles, which differ by a remarkable 23°. This is the most notable structural difference of the two diastereomers. The W−OR bond length and W−O−C bond angle are 1.835(8) Å and 159(1)° in the *S*-isomer and 1.858(7) Å and 134.8(8)° in the *R*- isomer. The shorter of the two W−OR distances is associated with a more obtuse W−O−C angle, a result consistent with somewhat greater oxygen lone-pair π-donation to tungsten from the alkoxide ligand in the *S*-isomer.[65] Structurally characterized oxo−thio−metal complexes are very rare, and the structures of *R*- and *S*-Tp*WOS{(−)-mentholate} are to our knowledge the first where potential oxo/thio disorder has been overcome by the incorporation of a chiral coligand. The structure is only the second nondisordered structure available for an oxo−thio−tungsten complex.

The structure of (*R,S*)-Tp*WOS{(−)-mentholate} is essentially molecular; however, an interesting mode of association between the *R*- and *S*-isomers occurs. Pseudocentrosymmetric pairs of molecules (with respect to the W centers) associate via W═O···H−C(35) interactions such that O(1a)···C(35b) is 3.51(2) Å and O(1b)···C(35a) is 3.49(2) Å. These separations correspond to O···H distances of 2.89 and 2.88 Å, respectively (note that the H atoms were included in their idealized positions).

Structure of $Tp^*WS_2(OPh)$. In $Tp^*WS_2(OPh)$, a distorted octahedral tungsten center is coordinated by a facial Tp* ligand, two terminal thio ligands, and a phenoxide ligand (Figure 2). The two W═S bond lengths (W−S(1) 2.131(4) Å; W−S(2) 2.129(4) Å) are equivalent and are close to the average established for bonds of this type (2.115 Å).[20−22,28−30] The short W═S bonds, the wide S(1)−W−S(2) angle (102.9(1)°), and large S(1)···S(2) distance (3.331(5) Å) establish the presence of a *cis*-$[W^{VI}S_2]^{2+}$ center and preclude the presence of, e.g., a $[W^{IV}(\eta^2\text{-}S_2)]^{2+}$ center.

The W−N bonds trans to the W═S groups (W−N(11) 2.268(8) Å; W−N(21) 2.272(9) Å) are experimentally equivalent and are longer than W−N(31) (2.161(9) Å), which lies trans to the

(60) Bands for $WOS(C_5H_{10}NO)_2$, 925 and 500 cm^{-1};[24] Cp*WOS(Me), 930 and 497 cm^{-1};[26] $Cp^*WOS(CH_2SiMe_3)$, 927 and 495 cm^{-1};[26] (L−N_2S_2)WOS, 928 and 492 cm^{-1};[29] $WOS(OSiPh_3)_2(Me_4phen)$, ν(WS) 480 cm^{-1}.[30]

(61) Similar bands are observed for related complexes: $Cp^*WS_2(Me)$, 499 and 495 cm^{-1};[26] $Cp^*WS_2(CH_2SiMe_3)$, 502 and 491 cm^{-1};[26] $Cp^*WS_2(S^tBu)$, 488 and 479 cm^{-1};[28] (L−N_2S_2)WS_2, 499 and 487 s cm^{-1};[29] $WS_2(OSiPh_3)_2(Me_4phen)$, $\nu(WS_2)$ 470 cm^{-1}.[30]

(62) (a) Roberts, S. A.; Young, C. G.; Cleland, W. E., Jr.; Ortega, R. B.; Enemark, J. H. *Inorg. Chem.* **1988**, *27*, 3044. (b) Roberts, S. A.; Young, C. G.; Kipke, C. A.; Cleland, W. E., Jr.; Yamanouchi, K.; Carducci, M. D.; Enemark, J. H. *Inorg. Chem.* **1990**, *29*, 3650. (c) Eagle, A. A.; Young, C. G.; Tiekink, E. R. T. *Organometallics* **1992**, *11*, 2934. (d) Xiao, Z.; Bruck, M. A.; Doyle, C.; Enemark, J. H.; Grittini, C.; Gable, R. W.; Wedd, A. G.; Young, C. G. *Inorg. Chem.* **1995**, *34*, 5950. (e) Laughlin, L. J.; Young, C. G. *Inorg. Chem.* **1996**, *35*, 1050. (f) Xiao, Z.; Bruck, M. A.; Enemark, J. H.; Young, C. G.; Wedd, A. G. *Inorg. Chem.* **1996**, *35*, 7508. (g) Eagle, A. A.; George, G. N.; Tiekink, E. R. T.; Young, C. G. *Inorg. Chem.* **1997**, *36*, 472.

(63) Cahn, R. S.; Ingold, C.; Prelog, V. *Angew. Chem., Int. Ed. Engl.* **1966**, *5*, 385.

(64) Nugent, W. A.; Mayer, J. M. *Metal−Ligand Multiple Bonds*; Wiley: New York, 1988; pp 157−158.

(65) Ashby, M. T. *Comments Inorg. Chem.* **1990**, *10*, 297.

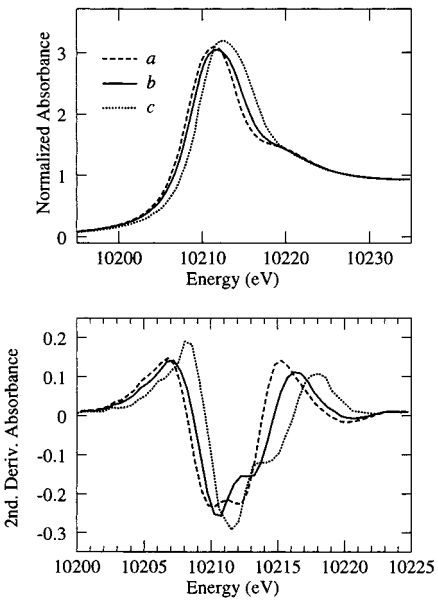

Figure 3. Tungsten L_{III} X-ray absorption near edge spectra (top) and second derivatives (bottom) for (a) Tp*WO_2Cl,[32,37] (b) Tp*WOSCl, and (c) Tp*WS_2Cl.

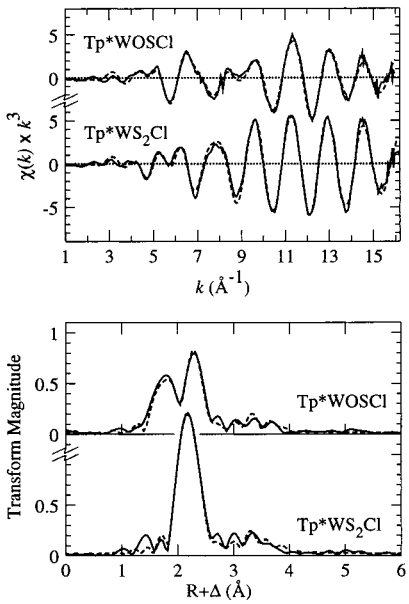

Figure 4. Tungsten L_{III} EXAFS (top) and Fourier transforms (bottom) for Tp*WOSCl and Tp*WS_2Cl. The experimental data are plotted as solid lines; the best fits, as dashed lines.[66]

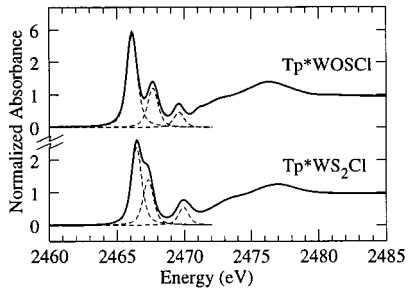

Figure 5. Sulfur K-edge X-ray absorption spectra of Tp*WOSCl and Tp*WS_2Cl. Deconvolution of the preedge regions yields the spectral components shown using the dashed lines.

phenoxide, reflecting the greater trans influence of the W═S ligands. The W−O(1) and W−N(31) vectors are inclined away from the thio ligands, and an O(1)−W−N(31) angle of 166.7-(2)° pertains. The W atom lies 0.9281(5) Å out of the plane defined by S(1), S(2), and O(1) and 1.4893(5) Å out of the plane defined by the N(*n*1) atoms. These structural features are shared by analogous dioxo−Mo and −W complexes.[37,62] Short M−OR bond lengths and M−O−C bond angles tending to linearity indicate alkoxide π-donation.[65] In this structure, the W−O bond length (1.889(8) Å) is typical of tungsten−alkoxides (1.900 Å),[22] and the W−O−C(41) bond angle (137.3(9)°) is clearly bent. These results suggest that the phenoxide ligand is not involved in significant π-donation to the $[W^{VI}S_2]^{2+}$ center and that the terminal thio ligands more strongly compete for empty metal d orbitals.

X-ray Absorption Spectroscopy. The W L_{III} X-ray absorption near-edge spectra of Tp*WO_2Cl, Tp*WOSCl and Tp*WS_2Cl are shown in Figure 3. All spectra exhibit an intense absorption around 10212 eV due to the dipole-allowed transitions from the $2p_{3/2}$ level to molecular orbitals involving the tungsten 5d manifold. Figure 3 also shows second derivative plots which reveal that the absorption is comprised of several peaks due to excitation into several d-orbital energy levels. The positions of the peaks were estimated by pseudo-Voigt peak deconvolution to be 10211.2 and 10214.3 eV for Tp*WO_2Cl, 10210.2 and 10213.3 eV for Tp*WOSCl, and 10209.8 and 10212.5 eV for Tp*WS_2Cl. The lowest energy peaks correspond to transitions to d orbitals close in energy to the LUMO of these W(VI) d^0 complexes. The peak separations give approximate (excited state) ligand-field splittings of 3.1, 2.9, and 2.7 eV for Tp*WO_2Cl, Tp*WOSCl, and Tp*WS_2Cl, respectively, broadly in line with expectations based on ligand field considerations.

Figure 4 shows the W L_{III} EXAFS oscillations and corresponding Fourier transforms and best fits for Tp*WOSCl and Tp*WS_2Cl. The EXAFS Fourier transform of Tp*WOSCl clearly shows two peaks, which are due to the W═O and overlapping W═S, W−Cl, and W−N interactions. Only a single peak, due to overlapping W═S, W−Cl, and W−N interactions, is observed in the EXAFS Fourier transform of Tp*WS_2Cl. Both transforms exhibit features above 3 Å due to the outer C and N shells of Tp*. The bond distances derived from curve-fitting analyses[66] are in excellent agreement with the parameters crystallographically determined for related species (vide supra). The W XAS/EXAFS results confirm the structural integrity of the chloro derivatives and provide electronic insights congruent with electrochemical results and bonding considerations (vide infra).

The sulfur K near-edge spectra of Tp*WOSCl and Tp*WS_2Cl are compared in Figure 5. Both spectra are dominated by very intense low-energy absorptions just above 2466 eV due to dipole-allowed transitions from the core level to excited states having substantial sulfur p- and metal d-orbital character, e.g., π^* and σ^* orbitals. Pseudo-Voigt deconvolution of the spectra gives accurate peak energies and intensities (in parentheses), which for the three lowest energy (and most intense) bands are

(66) The parameters used to fit the data are summarized below in the following format: backscatterer; coordination number *N*; interatomic distance *R*; (thermal and static) mean-square deviation in *R* (the Debye−Waller factor) σ^2. The values in parentheses are estimated standard deviations (precisions) obtained from the diagonal elements of the covariance matrix. We note that accuracies will be somewhat larger than the precisions, typically ±0.02 Å for *R* and ±20% for *N* and σ^2. For Tp*WOSCl, W═O, *N* 1, *R* 1.715(1) Å, σ^2 0.0012(1) Å^2; W═S, *N* 1, *R* 2.148(2) Å, σ^2 0.0014(3) Å^2; W−Cl, *N* 1, *R* 2.351(3) Å, σ^2 0.0022(3) Å^2; W−N, *N* 3, *R* 2.18(1) Å, σ^2 0.0089(2) Å^2. For Tp*WS_2Cl: W═S, *N* 2, *R* 2.142(1) Å, σ^2 0.0021(1) Å^2; W−Cl, *N* 1, *R* 2.364(2) Å, σ^2 0.0018(1) Å^2; W−N, *N* 3, *R* 2.23(1) Å, σ^2 0.0116(2) Å^2.

2466.12 (2.9), 2467.65 (1.2), and 2469.59 (0.47) eV for Tp*WOSCl and 2466.44 (2.4), 2467.31 (1.5), and 2469.74 (0.45) eV for Tp*WS_2Cl. All of these peaks are very sharp, having a full width at half-maximum of less than 0.8 eV, which is comparable to the 1s → π*($3b_1$) transition of gaseous SO_2 and indicative of transitions to single or degenerate levels. The spectrum of Tp*WOSCl is very similar to that of Tp^{Pr}-MoOS(OPh).[13] Monothio−Mo and −W complexes such as Tp*$MoSCl_2$,[67] Tp*$WSCl_2$, and their derivatives[68] exhibit subtlely different S K-edge spectra. For monothio complexes, the lowest energy band (ca. 2466 eV) is relatively broad and appears to be comprised of two transitions, possibly from excitations into nearly degenerate M═S π* levels. An absorption at intermediate energy, corresponding to the 2467.65 eV band of Tp*WOSCl, is absent from the spectra of monothio complexes; this supports the assignment of the Tp*WOSCl band to an excitation involving a W═S π* orbital with significant W═O π* character (vide infra). A small feature at ca. 2470 eV is observed in the spectra of all thio−Mo and −W complexes studied to date; it is tentatively ascribed to a transition to a σ* or pseudo-σ* orbital of mixed S p and d orbital character. A contraction in the energy range of the preedge features in the spectrum of Tp*WS_2Cl is consistent with a reduction in the energy range of the frontier π* LUMOs of the *cis*-$[WS_2]^{2+}$ unit. Full and confident assignment of complex spectra such as these normally requires polarized single-crystal experiments,[46] and their feasibility is currently being assessed.

Electrochemical Studies. Exchange of an oxo group for a thio group generally leads to a positive shift in M(VI)/M(V) (M = Mo, W) reduction potentials. This is illustrated by the potentials of the (irreversible) Mo(VI)/Mo(V) couples of $MoO_2(C_5H_{10}NO)_2$ (−2.50 V vs Fc^+/Fc[27] in DMF), $MoOS(C_5H_{10}NO)_2$ (−1.94 V), and $MoS_2(C_5H_{10}NO)_2$ (−1.59 V)[18] and the (reversible) Mo(VI)/Mo(V) couples of $Tp^{Pr}MoO_2$(OPh) (−0.78 V vs SCE in MeCN)[62d] and Tp^{Pr}MoOS(OPh) (−0.48 V).[13] Also, the complex $WO(S_2)(S_2CNEt_2)_2$ is more difficult to reduce (E_{pc} = −1.48 V vs Ag/AgCl) than the related thio complex $WS(S_2)(S_2CNBz_2)_2$ (E_{pc} = −1.04 V).[69] We note that $WS(S_2)(S_2CNBz_2)_2$ is reduced at the *same* potential as the related oxo−Mo(VI) complex $MoO(S_2)(S_2CNEt_2)_2$ (E_{pc} = −1.04 V),[69] consistent with results described below. Similar trends are observed in comparative electrochemical studies of oxo/thio complexes of other elements; e.g., thio ligation permits the observation of the Re(V)/Re(IV) couple of $[ReS(edt)_2]^-$, whereas reduction of $[ReO(edt)_2]^-$ was not achieved at accessible potentials.[54]

The cyclic voltammograms of Tp*WE_2X (E_2 = OS, S_2) were recorded in acetonitrile, and the data obtained are summarized in Table 5. A schematic representation of the potential ranges for the compounds Tp*WO_2X,[37] Tp*WOSX, Tp*WS_2X, and Tp*MoO_2X,[62d] is presented in Figure 6. The Tp*WOSX complexes generally undergo a reversible, one-electron reduction in the range −1.33 V to −0.84 V vs SCE. In the case of Tp*WOSCl, this process is electrochemically reversible at scan rates >200 mV•s^{-1} but only quasi-reversible at slower scan rates. The reduction of Tp*$WOS(S_2PPh_2)$ is irreversible at all scan rates. For reversible processes, peak-to-peak separations in the range 62−95 mV were consistent with one-electron reductions generating stable oxo−thio−W(V) anions, $[Tp^*WOSX]^-$. The mentholate complex, Tp*WOS{(−)-mentholate}, possesses the most negative reduction potential (−1.33 V), consistent with hard-donor stabilization of W(VI) and the finding that $E_{1/2}$ values for Tp*MoO_2(SR) become more positive as R becomes more electron-withdrawing; viz., $E_{1/2}$ is in the order R = 2° alkyl < 1° alkyl < aryl.[62d] The potentials for the X = EPh complexes, viz., OPh^- < SPh^- ~ $SePh^-$, are also consistent with greater stabilization of W(VI) by hard rather than soft donor coligands. Comparing $E_{1/2}$ or E_{pc} values as necessary, the reduction potentials of Tp*WOSX (X = Cl^-, OPh^-, SPh^-, $SePh^-$) are 330−440 mV (average 395 mV) more positive than those of their Tp*WO_2X analogues, the latter typically undergoing irreversible reductions at very negative potentials (from E_{pc} = −1.05 V for X = S_2PPh_2 to $E_{1/2}$ = −1.71 V for X = OMe^-).[37] The unusually small difference in reduction potentials of Tp*$WO_2(S_2PPh_2)$ and Tp*$WOS(S_2PPh_2)$ (ΔE = 140 mV, albeit for irreversible reductions) may indicate electronic buffering by the dithiophosphinate ligand or its involvement in a weak {W═S···S═P} interaction.[70] In summary, the replacement of a single oxo ligand in a $[WO_2]^{2+}$center by a thio ligand results in a dramatic positive shift in W(VI)/W(V) potentials.

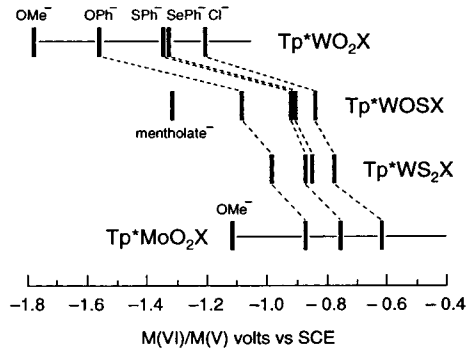

Figure 6. Comparison of M(VI)/M(V) redox potentials for Tp*ME_2X (M = Mo, W; E = O, S; X as specified) complexes in acetonitrile (except Tp*MoO_2Cl in CH_2Cl_2). The vertical bars represent the potentials of the specified X^- derivatives while the lighter horizontal bars represent the range of potentials for all Tp*MO_2X derivatives. See Table 5 and ref 62d for details.

The complexes Tp*WS_2X are reduced at potentials in the range −0.99 to −0.78 V vs SCE. These are 390−540 mV (average 450 mV) more positive than the potentials of the corresponding Tp*WO_2X complexes (the reduction potential of Tp*$WS_2(S_2PPh_2)$ is only 210 mV lower than the potential of Tp*$WO_2(S_2PPh_2)$). The differences in the reduction potentials of the Tp*WOSX and Tp*WS_2X (X = Cl^-, OPh^-, SPh^-, $SePh^-$, $S_2PPh_2^-$) complexes are in the range 30−100 mV (average 66 mV). This increase is much less than that associated with the first oxo-to-thio ligand conversion centered at Tp*WO_2X. The complexes Tp*WS_2X (X = OPh^-, SPh^-, and $SePh^-$) undergo a second irreversible reduction at E_{pc} = −1.53 to −1.55 V.

None of the complexes, except Tp*$WE_2(S_2PPh_2)$, undergo redox processes at positive potentials. The complexes Tp*$WE_2(S_2PPh_2)$ undergo a quasi-reversible oxidation at +0.73 V (E_2 = OS) and +0.75 (E_2 = S_2) leading to the generation of a trithiophosphinate−W(V) cation, $[Tp^*WE(S_3PPh_2)]^+$, via an

(67) Singh, R.; Spence, J. T.; George, G. N.; Cramer, S. P. *Inorg. Chem.* **1989**, *28*, 8.

(68) S K-edge XAS have been recorded for a series of complexes including Tp*$MoSX_2$ (X = Cl^-, OPh^-, *o*-$OC_6H_4Pr^-$, *o*-$OC_6H_4SEt^-$; X_2 = benzene-1,2-dithiolate, etc). All spectra exhibit preedge features at ca. 2466 and 2469 eV. Young, C. G.; Gable, R. W.; Hill, J. P.; George, G. N. *Eur. J. Inorg. Chem.* **2001**, 2227.

(69) Bond, A. M.; Broomhead, J. A.; Hollenkamp, A. F. *Inorg. Chem.* **1988**, *27*, 978.

(70) For a related example in molybdenum chemistry, see: Hill, J. P.; Laughlin, L. J.; Gable, R. W.; Young, C. G. *Inorg. Chem.* **1996**, *35*, 3447.

Table 5. Cyclic Voltammetric Data[a]

X	$E_{1/2}$ (V)	E_{pc} (V)	E_{pa} (V)	I_{pa}/I_{pc}	ΔE_{pp} (mV)	ΔE (mV) vs Tp^*WO_2X	ΔE (mV) vs Tp^*MoO_2X
				Tp^*WOSX			
Cl^-	−0.84	−0.88	−0.81	0.94	67	330[b]	−260[b,c]
$S_2PPh_2^-$	n/a	−0.91	n/a	n/a	n/a	140[b]	−450[b]
$SePh^-$	−0.92	−0.95	−0.88	0.89	69	390	
SPh^-	−0.93	−0.96	−0.88	0.95	85	390	−170
OPh^-	−1.09	−1.12	−1.06	1.02	62	470	−210
(−)-mentholate	−1.33	−1.38	−1.29	0.97	95		
				Tp^*WS_2X			
$S_2PPh_2^-$	n/a	−0.84	n/a	n/a	n/a	210	−380[b]
Cl^-	−0.78	−0.82	−0.75	0.54	70	390	−200[b,c]
SPh^-	−0.86	−0.89	−0.83	1.00	69	460	−100
$SePh^-$	−0.88	−0.92	−0.84	1.00	73	420	
OPh^-	−0.99	−1.03	−0.95	1.04	82	540	−110

[a] In MeCN, all processes reversible except the following: $Tp^*WOS(S_2PPh_2)$, irreversible; $Tp^*WS_2(S_2PPh_2)$, quasi-reversible; Tp^*WS_2Cl, quasi-reversible. n/a = not applicable. [b] Difference in E_{pc} values for quasi-reversible or irreversible reductions. [c] Tp^*MoO_2Cl in CH_2Cl_2.[62d]

induced internal redox process.[70] In line with this interpretation, a similar process is not observed for $Tp^*WO_2(S_2PPh_2)$.[37]

As previously reported, the reduction potentials of Tp^*WO_2X are an average 590 mV more negative than those of their Tp^*MoO_2X analogues (X = NCS^-, SPh^-, OPh^-, OMe^-).[37] In contrast, the reduction potentials of Tp^*WOSX and Tp^*WS_2X complexes are only 170−210 and 100−110 mV more negative, respectively, than those of Tp^*MoO_2X (X = SPh^-, OPh^-). Variation of X sees a significant overlap in the range of reduction potentials of Tp^*WOSX, Tp^*WS_2X, and Tp^*MoO_2X complexes (Figure 6) and it is clear that oxo−thio− and bis-(thio)−W(VI) complexes have one-electron reduction potentials broadly similar to those of their biologically relevant *cis*-$[MoO_2]^{2+}$ counterparts.

Reactivity. The reactivity of the title compounds is now briefly described. As reported previously,[37] complexes of the type Tp^*WO_2X do not participate in clean oxygen atom transfer (OAT) reactions with, e.g., phosphines. In contrast, the title compounds react rapidly with PPh_3 but sulfur atom transfer (SAT) rather than OAT takes place. This results in the formation of $SPPh_3$ and various tungsten compounds depending on the nature of the coligands and the solvent; e.g., reaction of Tp^*WOSCl with PPh_3 in pyridine results in the formation of $Tp^*WOCl(py)$ while the analogous reaction with Tp^*WS_2Cl produces $Tp^*WSCl(py)$. Addition of propylene sulfide to these W(IV) complexes regenerates the starting materials. The reactions of $Tp^*WOS(S_2PPh_2)$ and $Tp^*WS_2(S_2PPh_2)$ with PPh_3 result in the formation of $Tp^*WO(S_2PPh_2)$ and $Tp^*WS(S_2PPh_2)$, respectively.[47] These observations are consistent with the presence of strong W═O bonds and relatively weak W═S bonds in the complexes and the relative ease of reduction of the thio complexes compared to dioxo species. The potential of the complexes to act as SAT catalysts has been established in the case of Tp^*WS_2Cl; results relating to this aspect of their chemistry will be published elsewhere.

In contrast to related oxothiomolybdenum(VI) complexes, $Tp^*MoOS(S_2PR_2)$, the thiotungsten complexes do not react with cyanide to form thiocyanide. Thus, the inability of cyanide to deactivate some tungsten enzymes does not in itself establish the absence of thio ligation at tungsten. The bis(thio)tungsten complexes react with a variety of alkynes to produce dithiolene complexes of the type Tp*WX(dithiolene).[33,34,71]

Bonding Considerations. The stability and reactivity of the title compounds and their electrochemical behavior can be rationalized by simple bonding pictures. Take, for example, the complexes Tp^*WO_2Cl, Tp^*WOSCl, and Tp^*WS_2Cl, with idealized C_s or C_1 structures. For Tp^*WO_2Cl (C_s), a π-orbital manifold, comprising three 3-center π-orbitals ($2 \times a' + a''$), their π^* partners ($2 \times a' + a''$), and a nonbonding oxygen p orbital combination (a''), can be constructed from symmetry-adapted combinations of the four oxygen p_π and three tungsten d_π orbitals (Figure 7). The π-bonding orbitals are very stable and well below the energy of the frontier orbitals, consistent with strong W═O bonding. The $a'' \pi^*$ $[WO_2]$-based LUMO, which is comprised principally of the d_{xy} orbital, is at a relatively high energy. Consequently, the addition of an electron to this orbital causes considerable destabilization and is associated with a very negative reduction potential.[37] The high energy of the W═O π^* orbitals limits nucleophilic attack of the oxo ligands and effective OAT to reagents such as tertiary phosphines.[37]

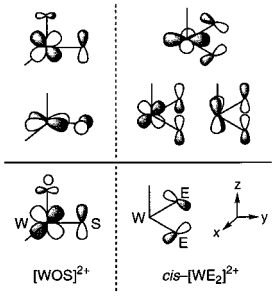

Figure 7. Qualitative representations of the frontier orbitals of the complexes Tp*WOSCl (left of dashed line) and Tp^*WE_2Cl (E = O, S) (right). The HOMO in each case is shown below the solid line, and the lowest energy π^* LUMOs are shown in the region above the solid line.

In Tp*WOSCl (C_1), the oxo ligand dominates the ligand field and the oxo π-bonding orbitals are well below the frontier orbital manifold. Here, the frontier orbitals are the π and π^* orbitals of the W═S unit (Figure 7). The HOMO is a 3-center [WOS]-based orbital which is antibonding with respect to W and O but bonding with respect to W and S; W d_{yz} and S p_z are the principal atomic orbitals involved in this interaction. The LUMO, a W═S π^* orbital involving W d_{xy} and S p_x atomic orbitals, is considerably lower in energy than the LUMO of Tp^*WO_2Cl. This accounts for the more positive reduction potentials observed for Tp^*WOSCl relative to Tp^*WO_2Cl. Nucleophilic attack at the more energetically accessible π^* W═S orbital, and the breaking of the weaker W═S bond (vs W═O) is consistent with the SAT reaction observed with PPh_3. The first two low-energy absorptions observed in the S K-edge

(71) Eagle, A. A.; George, G. N.; Tiekink, E. R. T.; Young, C. G. *J. Inorg. Biochem.* **1999**, *76*, 39.

spectrum of Tp*WOSCl may be due to transitions involving the two lowest energy π^* orbitals.

Metal−sulfur π interactions feature prominently in the frontier orbitals of Tp*WS_2Cl (Figure 7). The HOMO is expected to be the a″ combination of the in-plane S p orbitals of the WS_2 unit, and the LUMO, a three-center π^* orbital constructed from the W d_{xy} orbital and the a″ combination of S p_y orbitals. The LUMO is predicted to be only marginally lower in energy than the LUMO of Tp*WOSCl, accounting for the small but positive shift in the reduction potential of Tp*WS_2Cl compared to Tp*WOSCl. The reactivity of the thio ligands is consistent with the S p orbital character of the frontier orbitals.

Summary

Extended series of oxo−thio− and bis(thio)−W(VI) complexes, Tp*WOSX and Tp*WS_2X, have been prepared (using sulfidation, metathesis, and atom transfer reactions) and characterized by spectroscopic, electrochemical, and X-ray crystallographic studies. The stability of the compounds reflects the inability of the thio ligand (sulfide) to reduce W(VI); in contrast, the reduction of Mo(VI) by sulfide often thwarts attempts to synthesize thio−Mo(VI) complexes.[13,72,73] The crystal structures of (*R*,*S*)-Tp*WOS{(−)-mentholate} and Tp*WS_2(OPh) and the XAS/EXAFS studies of the chloro derivatives confirm the bis(chalcogenido) formulations. Electrochemical studies reveal that the complexes participate in reversible one-electron reductions, at potentials directly comparable to those of *cis*-$[MoO_2]^{2+}$ analogues and markedly more positive than the typically irreversible reductions of their *cis*-$[WO_2]^{2+}$ analogues. These findings highlight the capacity of terminal thio ligands to dictate the spectroscopic, chemical, and electrochemical properties of metal centers through modulation of the frontier (π/π^*) orbital manifold.

Acknowledgment. A.A.E. and C.G.Y. thank the Australian Department of Industry, Science and Technology for a travel grant permitting XAS measurements at SSRL. Financial support from the Australian Research Council is gratefully acknowledged. SSRL is funded by the Department of Energy (DOE) BES, with further support by DOE OBER and the National Institutes of Health.

Supporting Information Available: Tables of crystallographic data for (*R*,*S*)-Tp*WOS{(−)-mentholate} and Tp*WS_2(OPh)·CH_2Cl_2, infrared spectral data, and electrochemical data and representative cyclic voltammograms. This material is available free of charge via the Internet at http://pubs.acs.org.

IC010084S

(72) Eagle, A. A.; Laughlin, L. J.; Young, C. G.; Tiekink, E. R. T. *J. Am. Chem. Soc.* **1992**, *114*, 9195.

(73) Young, C. G. *J. Biol. Inorg. Chem.* **1997**, *2*, 810.